Appl. Phys. A (2014) 117:1491–1498
DOI 10.1007/s00339-014-8582-1

Applied Physics A
Materials Science & Processing

Local atomic arrangement in mechanosynthesized $Co_xFe_{1-x-y}Ni_y$ alloys studied by Mössbauer spectroscopy

Tomasz Pikula

Received: 18 December 2013 / Accepted: 1 July 2014 / Published online: 17 July 2014

Abstract Mechanosynthesized $Co_xFe_{1-x-y}Ni_y$ alloys were examined using X-ray diffraction (XRD) and Mössbauer spectroscopy. In order to explain the shape of hyperfine magnetic field (HMF) distributions for the alloys, a local environment model based on a multinomial distribution was proposed. The model was in agreement with the XRD data and confirmed that the studied alloys were disordered solid solutions. It was successfully applied to describe the samples with *bcc* and *fcc* crystalline lattice type within the relatively broad range of components concentration. The results showed that the change of the crystalline lattice type does not cause an abrupt change of the HMF value. Moreover, a mean number of unpaired spins for the first coordination sphere may be used as a parameter to describe the HMF value experienced by ^{57}Fe nucleus. Finally, a set of the most probable atomic configurations and their corresponding contributions to the HMF distribution were obtained.

1 Introduction

It is well known that many of the physical properties of alloys depend on local atomic arrangement of atoms in crystalline lattice. During the past few decades, many efforts were made to examine the type of atomic ordering in a variety of materials. Mössbauer spectroscopy, X-ray diffraction (XRD) and neutron diffuse scattering were the most commonly used techniques for this purpose [1, 2].

When considering the chemical ordering of atoms, three types of alloys can be distinguished: (1) disordered systems, (2) alloys with a short-range order (SRO) and (3) alloys with a long-range order (LRO). The disordered state means that atoms of individual components are randomly located at lattice sites, and the probability of finding a given type of atom in a particular crystallographic position is simply given by the chemical concentration of such element. The term short-range order is used to describe the preference of certain types of atoms to reside near each other. The long-range order is related to the development of a certain atomic pattern through the whole crystal [3].

Quantitatively, the effect of atomic ordering can be described by the short-range order parameters, also called Warren-Cowley parameters [4]. In binary $A_{1-x}B_x$ alloys, they can be expressed by following formula:

$$\alpha_i = 1 - \frac{P_i(B)}{x}, \tag{1}$$

where $P_i(B)$ is an experimentally determined probability of finding the B-type atom in i-th coordination zone around the A atom and x is the chemical concentration of B component. The values of α_i parameters are a measure of the deviation from the random state and equal zero for completely disordered systems [5]. Positive α_i value means that the atoms on the neighboring atomic sites are more likely to be of the same atomic species. Such type of concentration fluctuation is called clustering. Negative value of SRO parameters occurs when there is energetic preference of unlike pairs of atoms to occupy adjacent atomic sites. This type of order, referred to as anti-clustering, if extended on longer-range correlations, leads to the superstructure formation [2].

T. Pikula (✉)
Faculty of Electrical Engineering and Computer Science,
Institute of Electronics and Information Technology, Lublin
University of Technology, Nadbystrzycka Str. 38A,
20-618 Lublin, Poland
e-mail: t.pikula@pollub.pl

Mössbauer spectroscopy is one of the most suitable experimental methods, which can be used to determine the type of ordering in alloys. It is well suited especially for Fe-containing magnetic systems where the HMF induction can be used as the main spectral parameter [6, 7]. In the case of binary $Fe_{1-x}A_x$ disordered alloys, probability distributions of HMF values are observed. They reflect an occurrence of different atomic configurations in the nearest neighborhood of ^{57}Fe atoms. Each configuration produces distinct HMF value, B_{hf}, experienced by ^{57}Fe nuclei and can be described in terms of the additive model as [4, 5, 8–10]:

$$B_{hf} = B_{Fe} + n\Delta B \tag{2}$$

where B_{Fe} is the value of HMF for pure Fe, n is the number of impurity atoms in the first coordination sphere and ΔB denotes a change of the HMF caused by a single impurity atom A.

From the statistical point of view, for a completely random binary alloy given by the formula $Fe_{1-x}A_x$, the probability of finding n of A-type atoms in the nearest neighborhood of Fe atom can be calculated using binomial distribution [11]:

$$P(n) = \frac{N!}{n!(N-n)!}(1-x)^n x^{N-n} \tag{3}$$

where N is the number of all atoms in the first coordination sphere and x denotes the chemical concentration of the A component in the alloy. Comparison of the shape of binomial distribution given by Eq. (3) with experimental HMF distribution obtained through numerical fitting of the Mössbauer spectra makes it possible to conclude about presence, or lack of atomic ordering in the alloy. This can be done quantitatively in terms of the SRO parameters defined by the formula (1).

The Mössbauer spectra analysis of disordered and ordered at short-range scale alloys was widely discussed for a variety of binary systems, e.g., Fe–Al, Fe–W [8], Fe–Ti [5], Fe–Mo [9], Fe–Mn [12], Fe–Cr [13], Fe–V [14], Fe–Ni, Fe–Co [15]. On the other hand, not many investigations were done to explain the shape of HMF distributions in the case of ternary alloys. The aim of this work is to provide an interpretation of the shape of HMF distributions for a series of $Co_xFe_{1-x-y}Ni_y$ alloys prepared by mechanical alloying (MA). As it was proved by several authors [16–19], the $Co_xFe_{1-x-y}Ni_y$ alloys exhibit soft magnetic properties and can be used as a head core material in magnetic storage devices.

2 Experiment

A series of twelve $Co_xFe_{1-x-y}Ni_y$ alloys was prepared by MA in Fritsch P5 planetary ball mill. Synthesis of the samples was carried out in an argon atmosphere and finished after 100 h of milling. The compositions of the alloys chosen for investigation are shown in Table 1. In order to describe the structure of prepared samples, XRD on Philips PW 1830 diffractometer was applied. Mössbauer spectroscopy measurements were carried out with the POLON spectrometer, which was working in a constant acceleration mode. The ^{57}Co was used as the radiation source of gamma quanta. Scanning electron microscopy and energy-dispersive X-ray spectroscopy studies were carried out to examine the homogeneity of the alloys. Detailed information about experimental techniques and their results can be found in the previous works of the author, i.e., [20–22].

Table 1 Selected structural and hyperfine interactions parameters of mechanosynthesized $Co_xFe_{1-x-y}Ni_y$ alloys: D—average grain size, $\langle B_{hf}\rangle$—mean HMF induction, B_{max}—most probable HMF induction, $\langle s\rangle$—average number of unpaired spins per atom in the first coordination sphere [the average of the statistical $P(s)$ distribution, formula (8)]

Alloy	Lattice	D (nm)	$\langle B_{hf}\rangle$ (T)	B_{max} (T)	$\langle s\rangle$
$Co_{40}Fe_{60}$	*bcc*	50 (40)	35.45	35.57	3.6
$Co_{40}Fe_{50}Ni_{10}$	*bcc*	60 (30)	34.36	34.47	3.4
$Co_{50}Fe_{45}Ni_5$	*bcc*	20 (20)	33.90	34.15	3.4
$Co_{40}Fe_{45}Ni_{15}$	*bcc*	20 (20)	33.88	33.89	3.3
$Co_{50}Fe_{40}Ni_{10}$	*bcc*	15 (1)	31.38	33.19	3.3
$Co_{60}Fe_{35}Ni_5$	*bcc*	40 (30)	33.50	33.44	3.3
$Co_{40}Fe_{40}Ni_{20}$	*bcc*	36 (1)	33.10	33.19	3.2
$Co_{50}Fe_{35}Ni_{15}$	*bcc*	60 (30)	33.06	33.08	3.2
$Co_{60}Fe_{30}Ni_{10}$	*bcc*	60 (30)	32.94	32.93	3.2
$Co_{65}Fe_{23}Ni_{12}$	*fcc*	10 (1)	30.63	32.06	3.11
$Co_{40}Fe_{35}Ni_{25}$	*fcc*	20 (15)	32.76	32.79	3.1
$Co_{52}Fe_{26}Ni_{22}$	*fcc*	24 (1)	32.20	32.32	3.04

3 Results and discussion

In the process of MA, one-phase $Co_xFe_{1-x-y}Ni_y$ alloys were obtained. They were in powder state, with the average particle size of 10–20 μm. As was proved by XRD measurements, the particles were of nanocrystalline structure and consisted of crystalline grains with a mean size of 10–60 nm. The alloys were disordered solid solutions, characterized by the *bcc*, or *fcc* crystalline lattice of the regular system. Detailed structural investigations were presented earlier in works [23–26].

Figure 1a presents, as an example, room-temperature Mössbauer spectra for mechanosynthesized $Co_{40}Fe_{40}Ni_{20}$ system, recorded at various stages of milling process. They were numerically fitted using Hesse–Rübartsch HMF distribution method [27] under assumption that each spectrum is a superposition of a certain number of sextets,

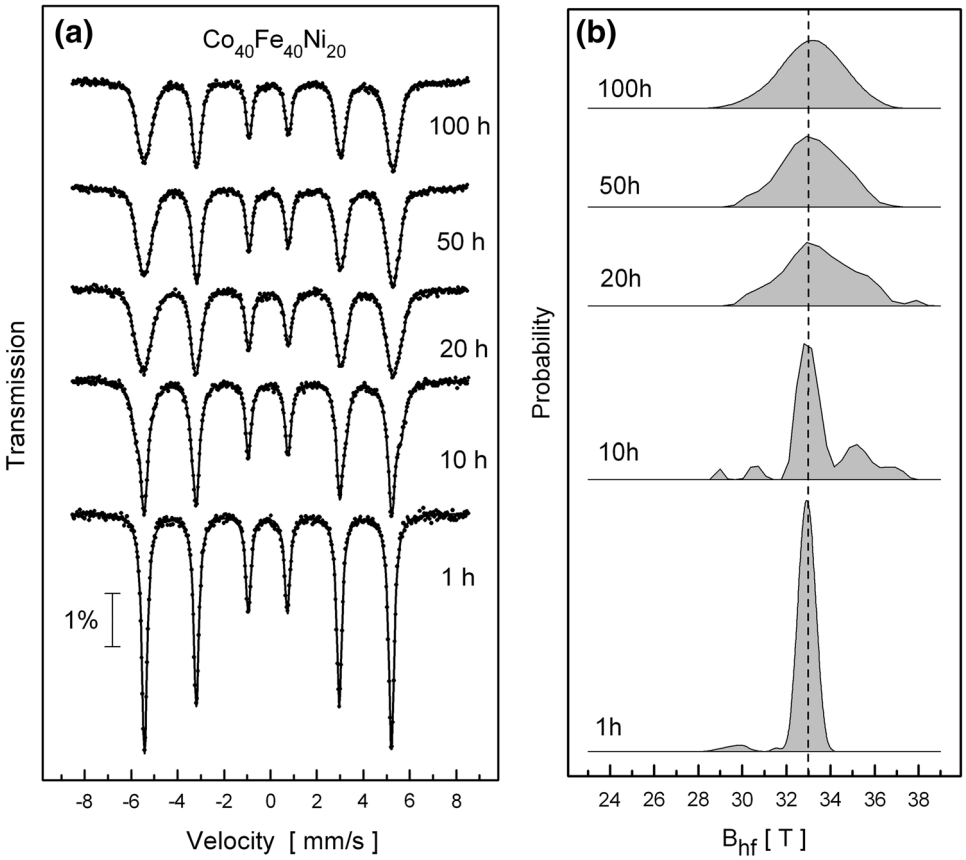

Fig. 1 **a** Room-temperature Mössbauer spectra and **b** HMF distributions of the mechanosynthesized $Co_{40}Fe_{40}Ni_{20}$ alloy for various milling periods

corresponding to various atomic configurations in the nearest neighborhood of ^{57}Fe atoms (distributions are shown in Fig. 1b). Linear correlation between the values of isomer shift (IS) and HMF, as well as between the quadruple splitting (QS) and HMF was assumed. It can be noted that with the increase of the time of milling, a significant broadening of the spectral lines occurs (Fig. 1a). After 1 h of milling (Fig. 1b), the 33 T-component connected with metallic iron is visible. The broadening of the distribution at this stage results mainly from increasing level of lattice deformations and strains. Such situation is typical for plastic deformation stage of mechanical alloying. It can be expected that the mutual interdiffusion of Co, Fe and Ni atoms starts after few hours of milling, when the level of internal strains significantly increases and the contact area of components is sufficient. Therefore, after 10 h of milling, in addition to the main 33 T-component, peaks with distinct HMF fields appear. On the basis of the HMF values given for binary alloys [28, 29], one can expect that the high-field peaks (34–37 T) are related to the presence of binary CoFe-based systems, while the low-field ones (26–32 T) are connected with the formation of FeNi and CoNi systems. Further increase of an area of the lateral maxima and their shifting toward main peak can be observed up to about 50 h. This is a clear evidence of atom mixing, i.e., ^{57}Fe probe atoms start to sense the presence of different atomic configurations around it, according to the alloy composition. The analyses of XRD patterns shown in [21] and [30], as well as shape of HMF distributions allow to conclude that the unification of the crystalline lattice type occurs after about 40–50 h of mechanosynthesis. Small irregularities of HMF distributions at this stage may indicate a lack of homogeneity of the alloy. For most of the studied samples, formation of a homogenous disordered solid solution occurs after 80–100 h of milling. Then in the Mössbauer spectrum, the sextets with broadened external lines typical for disordered ferromagnetic materials can be observed.

Hyperfine magnetic field distributions obtained for the final products of mechanosynthesis are shown in Fig. 2. Parameters of the experimental distributions, such as most probable HMF, B_{max}, and mean HMF, $<B_{hf}>$, are listed in Table 1. It is important to note that all of the presented curves are regular and have Gaussian-like shape, except for $Co_{50}Fe_{40}Ni_{10}$, $Co_{65}Fe_{23}Ni_{12}$ alloys. These are the most fine-grained samples with the average grain size, D, of 15 and 10 nm, respectively. Using the coherent polycrystal model [31] and assuming that the average grain boundary thickness is about 1 nm [30], it can be estimated that for the samples mentioned above, about 20–30 % of atoms is

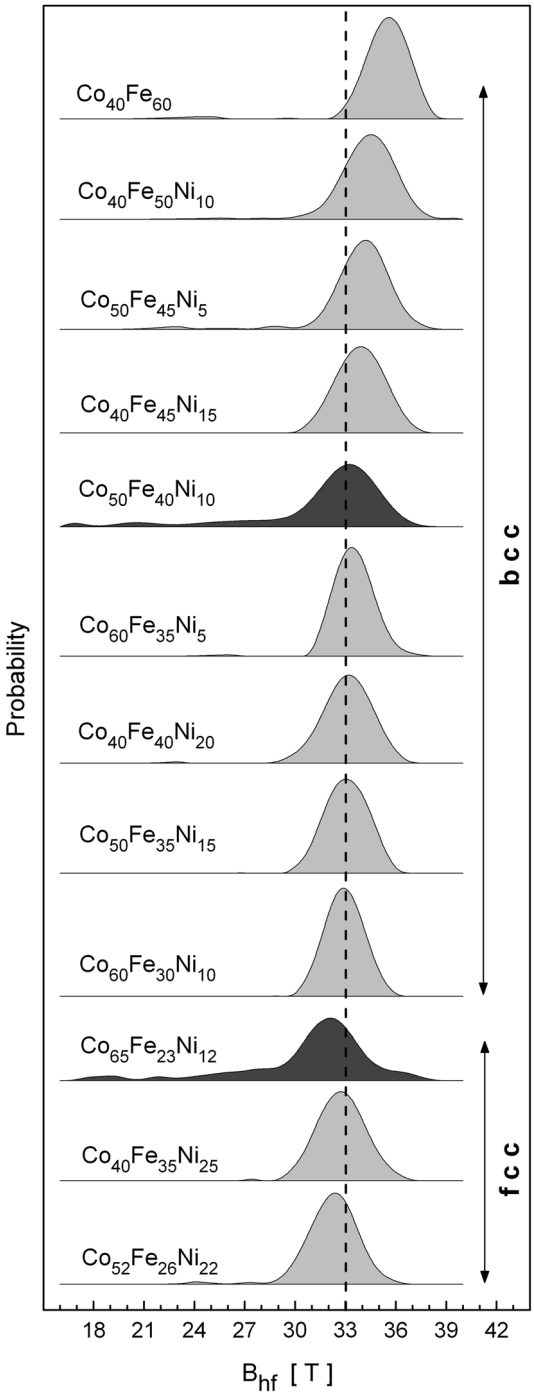

Fig. 2 Hyperfine magnetic field distributions for final products of milling process. The *dashed line* indicates the 33 T—HMF value for pure iron. The samples with the average grain size below 15 nm were marked with the *darkest color*

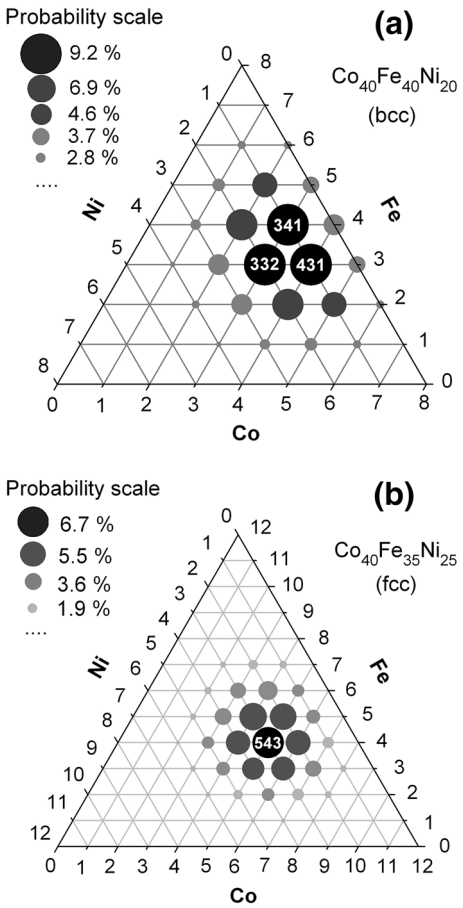

Fig. 3 Results of the calculations of atomic configurations probability $P(n, m)$ obtained according to formula (4) for **a** $Co_{40}Fe_{40}Ni_{20}$ and **b** $Co_{40}Fe_{35}Ni_{25}$ alloys

located within the grain boundary area. A relatively large increase in the volume of structurally disordered grain boundaries causes broadening of the experimental HMF peak and a significant contribution of low-field background in the total HMF distribution. Interestingly, when analyzing the position of curves shown in Fig. 2, one can note that the change of the crystalline lattice type does not cause an abrupt change in the B_{max} value.

Statistically, the probability of finding n of Co atoms and m of Ni atoms in the first coordination shell of ^{57}Fe atoms in $Co_xFe_{1-x-y}Ni_y$ alloy can be calculated using multinomial distribution [32]:

$$P(n,m) = \frac{N!}{n!\,m!\,(N-n-m)!}\; x^n\; y^m (1-x-y)^{(N-n-m)} \tag{4}$$

where N is the number of all atoms in the first coordination zone (8 for *bcc* and 12 for *fcc*).

For the *bcc* lattice, 45 different atomic configurations in the first coordination shell are possible, while for *fcc* lattice, the number reaches 91. The results of the statistical calculations can be visualized on the plane of Gibbs triangle similar to the phase equilibrium diagram (Fig. 3). This time, the axes are not marked with the chemical concentrations of components, but with a number of atoms of individual component in the first coordination sphere. As

an example, Fig. 3 shows the results of calculations performed for *bcc*-$Co_{40}Fe_{40}Ni_{20}$ and *fcc*-$Co_{40}Fe_{35}Ni_{25}$ alloys. Each intersection of lines in the triangle indicates a possible atomic configuration (*n q m*), where *n* is the number of Co atoms, *q*—Fe atoms and *m*—Ni atoms. The most probable configurations are marked by the greatest symbols, whereas the lack of a symbol indicates the probability of <1 %. It can be noted that for $Co_{40}Fe_{35}Ni_{25}$ alloy, the most probable configuration is (543), while for $Co_{40}Fe_{40}Ni_{20}$ alloy, there are three most probable configurations, i.e., (341), (332), (431).

The statistical distribution of probability given by formula (4) and visualized by Fig. 3 is a function of two arguments (*n*, *m*). On the other hand, the HMF distribution obtained from Mössbauer spectra analysis is a function of one parameter (B_{hf}). Therefore, direct comparison of such distributions is impossible. At first glance, individual values of B_{hf} may be attributed to suitable atomic configurations as it was done previously for binary alloys [29, 30]. Such reasoning leads to the theoretical distribution with broad and flat maximum, e.g., for $Co_{40}Fe_{40}Ni_{20}$ alloy where three different atomic configurations are equally probable. This result strongly disagrees with experimental data (Fig. 2). Another idea applied by Łopuszyński [3] is to describe ternary alloys as a quasi-binary alloys, i.e., to consider small amount of Ni as a perturbation of Co-Fe system. The limitation of this method is that it can be used only for alloys with a small concentration of Ni and only within the same type of crystalline lattice.

The reliable way to explain the shape of HMF distributions in the case of ternary $X_xFe_{1-x-y}Y_y$ alloys was reported by the authors of [1, 10, 32]. They used the additive model in accordance with formula (2), generalized for ternary alloys. According to the model, a certain atomic configuration (*n*, *q*, *m*) in the nearest neighborhood of ^{57}Fe probe produces HMF value described by the following expression:

$$B_{\mathrm{hf}} = B_{\mathrm{Fe}} + n\Delta B_1 + m\Delta B_2 \tag{5}$$

where *n*, *q*, *m* are the numbers of atoms of X, Fe and Y components in the first coordination sphere, while ΔB_1 and ΔB_2 denote changes of the HMF caused by a single X, or Y impurity atom. The weak point of such reasoning was that the ΔB_1 and ΔB_2 were parameters chosen empirically, and their values were changed accordingly to the composition of alloys. Nevertheless, high goodness of HMF fitting was achieved in some cases.

Instead of using *n* and *m* parameters to describe the shape of HMF distributions for $Co_xFe_{1-x-y}Ni_y$ alloys, the author of the present work proposes to introduce a new parameter, namely the average number of unpaired spins for the first coordination sphere, *s*, given by the formula:

Table 2 Calculations of probability $P(n, m)$ of different atomic configurations in the first coordination sphere and their mean numbers of unpaired spins, *s*, for *bcc*-$Co_{40}Fe_{40}Ni_{20}$ alloy

n	*q*	*m*	*P*(*n*, *m*)	*s*
3	4	1	9.17	3.375
4	*3*	*1*	*9.17*	*3.25*
3	3	2	9.17	3.125
2	*4*	*2*	*6.88*	*3.25*
4	2	2	6.88	3
2	5	1	5.5	3.5
5	2	1	5.5	3.125
4	4	0	4.58	3.5
2	3	3	4.58	3
3	2	3	4.58	2.875
3	5	0	3.67	3.625
5	3	0	3.67	3.375
1	5	2	2.75	3.375
5	1	2	2.75	2.875
1	4	3	2.29	3.125
4	1	3	2.29	2.75
2	6	0	1.83	3.75
1	6	1	1.83	3.625
6	*2*	*0*	*1.83*	*3.25*
6	1	1	1.83	3
1	3	4	1.14	2.875
3	1	4	1.14	2.625

The configurations with probabilities <1 % were not included in the table. Selected magnetically equivalent configurations were italicized

$$s = \frac{ns_{\mathrm{Co}} + qs_{\mathrm{Fe}} + ms_{\mathrm{Ni}}}{N} \tag{6}$$

where $s_{\mathrm{Co}} = 3$, $s_{\mathrm{Fe}} = 4$, $s_{\mathrm{Ni}} = 2$ represent theoretical number of unpaired 3*d* electrons for suitable components. Since Co, Fe and Ni are characterized by similar values of the atomic radius and all of them exhibit the 3*d*-type magnetism, one can suppose that the values of HMF sensed by the ^{57}Fe nuclei in a specific chemical surrounding depend on *s* value only. Therefore, the *s* value was calculated for each possible atomic configuration. As an example, Table 2 shows results of $P(n, m)$, and *s* calculations performed for *bcc*-$Co_{40}Fe_{40}Ni_{20}$ alloy. One can note that some of the configurations [e.g., (431), (242), (620) italicized in Table 2] are characterized by the same *s* value. It can be assumed that they produce the same HMF value at the ^{57}Fe site and can be therefore called magnetically equivalent. The probabilities of magnetically equivalent configurations were summed as follows:

$$P(s) = \sum_{i=1}^{k} P_i(n, m) \tag{7}$$

where *k* denotes the number of magnetically equivalent configurations. Figure 4 presents the distributions of probability, $P(s)$, calculated for *bcc*-$Co_{40}Fe_{40}Ni_{20}$ and *fcc*-$Co_{40}Fe_{35}Ni_{25}$ alloys, respectively. The same method was

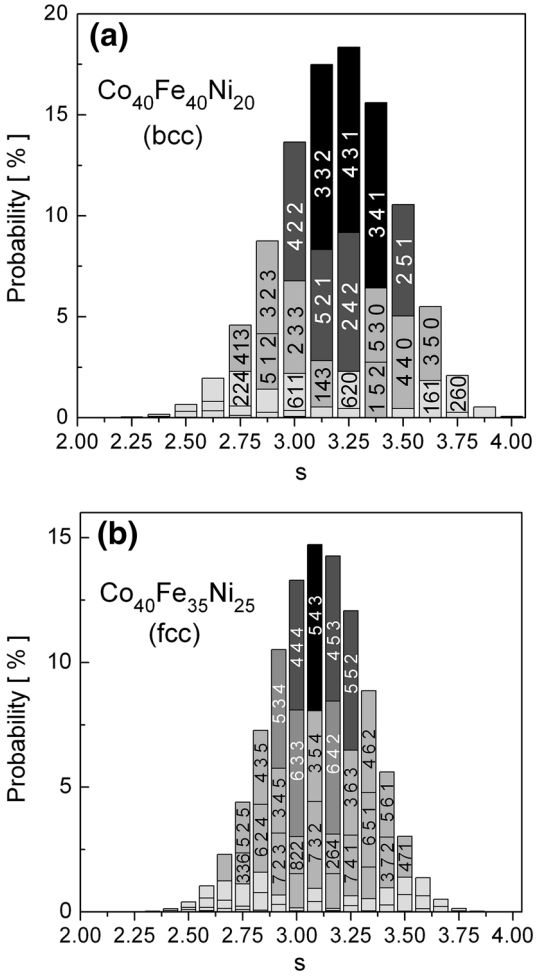

Fig. 4 The probability $P(s)$ of occurrence of mean number of unpaired spins, s, for the first coordination sphere for **a** *bcc*-$Co_{40}Fe_{40}Ni_{20}$ and **b** *fcc*-$Co_{40}Fe_{35}Ni_{25}$ alloys. The configurations with the highest probability were labeled

applied for all investigated alloys, and Gaussian-type distributions were obtained. Thus, the multinomial distributions $P(n, m)$ obtained for the series of mechanosynthesized $Co_xFe_{1-x-y}Ni_y$ alloys were transformed to the $P(s)$ form.

The next step of the proposed method is to compare the experimentally obtained HMF distribution with theoretically calculated statistical distribution, $P(s)$. For each value of the average number of unpaired spins calculated from $P(s)$ distribution:

$$<s> = \sum_{i=1}^{l} P(s_i) \cdot s_i \tag{8}$$

the most probable experimental HMF, B_{max}, was attributed as presented in Fig. 5 and Table 1. The l stands for the number of all possible s values for each alloy. Linear correlation between B_{max} and $<s>$ values is proved by Pearson's correlation factor, $R = 0.983$ and may be described by the function:

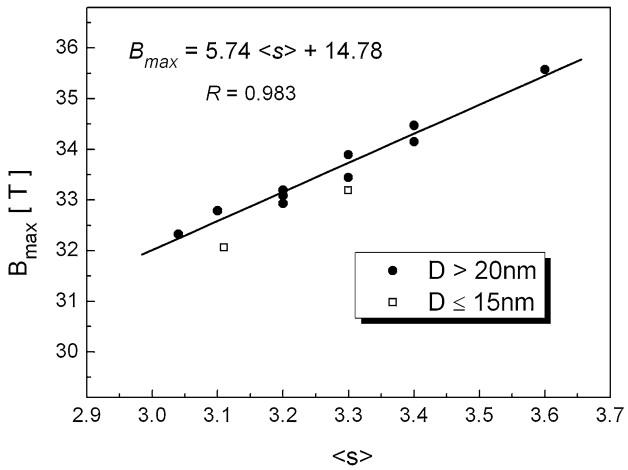

Fig. 5 The dependence of the most probable HMF value on the average number of unpaired spins for the first coordination sphere for mechanosynthesized $Co_xFe_{1-x-y}Ni_y$ alloys. R denotes the Pearson's correlation factor

$$B_{max} = 5.74 <s> + 14.78 \tag{9}$$

It can be stated that with each unpaired spin, the value of the HMF increases by the rate of 5.74 T. The biggest deviation from this tendency can be observed in the case of the two most fine-grained samples ($D \leq 15$ nm).

The formula (9) was used to convert all of the $P(s)$ statistical distributions to $P(B_{hf})$ HMF distributions. Moreover, the $P(B_{hf})$ and $P(s)$ functions were normalized to the unitary area. Figure 6 illustrates the results of transformation and allows to qualitatively compare both groups of distributions. Despite the fact that it was considered only the influence of the nearest neighbors of ^{57}Fe, high goodness of fitting was achieved. Some discrepancies may be caused by dispersion of the crystalline grain sizes, D (see Table 1), as well as by the significant level of internal strains and deformations occurring during mechanical alloying. It is worth noting that the presented model provides explanation for the shape of HMF distributions within a relatively broad range of chemical concentration of components and is applicable to alloys with both *bcc* and *fcc* lattice. Furthermore, it confirms that in the case of the studied $Co_xFe_{1-x-y}Ni_y$ samples, the atoms of components are arranged in a statistical manner. However, it should be mentioned that the presented parameterization has a heuristic character, and its main purpose is to satisfactorily account for the studied $Co_xFe_{1-x-y}Ni_y$ solid solutions.

4 Conclusions

On the basis of the performed studies, it can be stated that all the investigated $Co_xFe_{1-x-y}Ni_y$ alloys were disordered solid solutions. Simple model based on multinomial

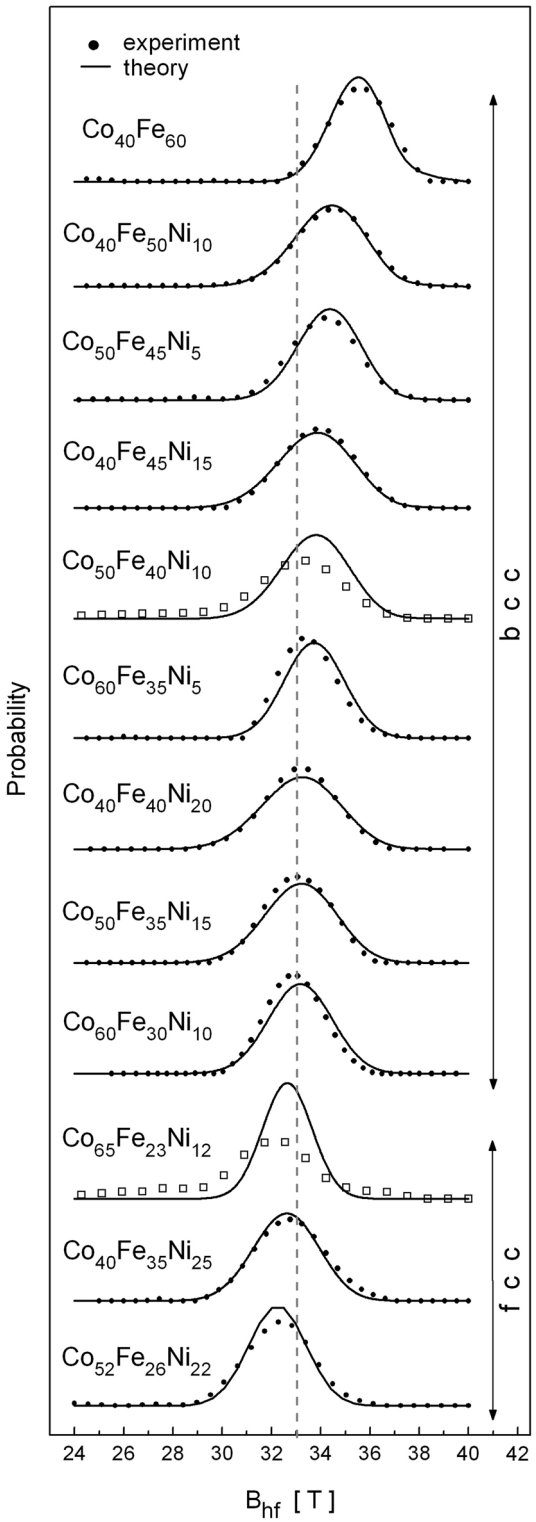

Fig. 6 Comparison of the HMF distributions obtained from Mössbauer measurements with the distributions calculated theoretically

distribution was successfully applied to explain the shape of HMF distributions in the case of ternary $Co_xFe_{1-x-y}Ni_y$ samples. The change of the crystalline lattice type from *fcc* to *bcc* does not cause a rapid change of the HMF value. The parameter which may be used to describe the value of HMF sensed by ^{57}Fe probe is the mean number of unpaired spins, *s*, for the atom in the first coordination shell. Center of the experimental distribution shifts toward higher HMF proportionally to the mean *s* value. Significant broadening of HMF distributions and rapid change of the values of hyperfine interactions parameters were observed in the case of the samples with average grain size bellow 15 nm. Such effect is related to the large contribution of grain boundaries in the total volume of the sample. The method of HMF distribution analysis presented in this paper can be used to investigate local atomic order in the case of ternary $Co_xFe_{1-x-y}Ni_y$ system, and it may help to monitor the process of mechanosynthesis. Moreover, it can be easily extended on higher number of coordination spheres, which will be the subject of further investigations of the author.

Acknowledgments Tomasz Pikula is a participant of the project: "Qualifications for the labour market—employer friendly university," co-financed by European Union from European Social Fund.

References

1. C. Djega-Mariadassou, L. Bessais, C. Servant, Phys. Rev. B **51**, 8830 (1995)
2. J.L. Robertson, C.J. Sparks, G.E. Ice, X. Jiang, S.C. Moss, L. Reinhard, in *Local Structure from Diffraction*, ed. by S.J.L. Billinge, M.F. Thorpe (Plenum Press, New York, 1998), p. 175
3. M. Łopuszyński, J.A. Majewski, Phys. Rev. B **85**, 35211 (2012)
4. J.M. Cowley, Phys. Rev. **77**, 669 (1950)
5. J. Cieślak, S.M. Dubiel, J. Alloy. Compd. **387**, 36 (2005)
6. M. Wiertel, Z. Surowiec, M. Budzyński, A.V. Tsvyashchenko, Acta Phys. Pol., A **114**, 1517 (2008)
7. Z. Surowiec, M. Wiertel, A.I. Beskrovnyi, J. Sarzynski, J.J. Milczarek, J. Phys.: Condens. Matter **15**, 6403 (2003)
8. E. Jartych, J. Magn. Magn. Mater. **265**, 176 (2003)
9. R. Idczak, R. Konieczny, J. Chojcan, Hyperfine Interact. **208**, 1 (2012)
10. J.M. Greneche, J. Non-Cryst, J. Non-Cryst. Solids **287**, 37 (2001)
11. J. Chojcan, J. Alloy. Compd. **264**, 50 (1998)
12. J. Chojcan, G. Roztocka, Phys. Stat. Sol. B **204**, 829 (1997)
13. J. Chojcan, Phys. Stat. Sol. B **219**, 375 (2000)
14. J. Chojcan, J. Alloy. Compd. **350**, 62 (2003)
15. R. Idczak, R. Konieczny, Z. Konieczna, J. Chojcan, Acta Phys. Pol., A **119**, 37 (2011)
16. T. Osaka, Electrochim. Acta **45**, 3311 (2000)
17. S.U. Jen, H.P. Chiang, C.M. Chung, M.N. Kao, J. Magn. Magn. Mater. **236**, 312 (2001)
18. E.V. Khomenko, E.E. Shalyguina, N.G. Chechenin, J. Magn. Magn. Mater. **316**, 451 (2007)
19. E.I. Cooper, C. Bonhote, J. Heidmann, Y. Hsu, P. Kem, J.W. Lam, M. Ramasubramanian, N. Robertson, L.T. Romankiw, H. Xu, IBM J. Res. Dev. **49**, 103 (2005)

20. T. Pikula, D. Oleszak, M. Pękała, E. Jartych, Acta Phys. Pol., A **114**, 1545 (2008)
21. T. Pikula, D. Oleszak, M. Pękała, J.K. Żurawicz, E. Jartych, Rev. Adv. Mater. Sci. **18**, 322 (2008)
22. T. Pikula, D. Oleszak, M. Pękała, E. Jartych, J. Non-Cryst. Solids **354**, 4267 (2008)
23. T. Pikula, D. Oleszak, E. Jartych, J. Phys: Conf. Ser. **217**, 012082 (2010)
24. T. Pikula, Nukleonika **58**, 151 (2013)
25. T. Pikula, D. Oleszak, M. Pękała, Acta Phys. Pol., A **119**, 52 (2011)
26. E. Jartych, J. Magn. Magn. Mater. **323**, 209 (2011)
27. J. Hesse, A. Rübartsch, J. Phys. E: Sci. Instrum. **7**, 526 (1974)
28. E. Jartych, J. Olchowik, J.K. Żurawicz, M. Budzyński, J. Phys.: Condens. Matter **5**, 8921 (1993)
29. E. Jartych, J.K. Zurawicz, D. Oleszak, M. Pękała, Nanostruct. Mater. **12**, 927 (1999)
30. E. Jartych, D. Oleszak, M. Pękała, J. Sarzyński, M. Budzyński, J. Mater. Sci. **39**, 5385 (2004)
31. H.W. Song, S.R. Guo, Z.Q. Hu, Nanostruct. Mater. **11**, 203 (1999)
32. J. Restrepo, G.A. Perez Alcazar, J. Magn. Magn. Mater. **213**, 135 (2000)